Analytical Methods

ROYAL SOCIETY OF CHEMISTRY

PAPER

View Article Online
View Journal

Cite this: DOI: 10.1039/d4ay01431f

A DMSO-assisted iridium(III) complex as a luminescent "turn-on" sensor for selective detection of L-histidine and bacterial imaging†

Xiaojuan Li,[a] Tianqian Jia,[a] Yueyan Wang,[a] Yanyan Zhang,[a] Du Yang,[a] Sicheng Zhai[a] and Shuming Li *[b]

Histidine (His) is a semi-essential amino acid and a unique key neurotransmitter involved in numerous physiological processes. An excessive or deficient amount of His in the body can lead to various related diseases. However, since the chemical structures of L-His and its metabolites (such as histamine (Ha), imidazole-4-acetate (ImA), *etc.*) are very similar, simple and efficient selective detection of L-His and its related metabolites is of great importance but remains a great challenge. Herein, we successfully designed and synthesized a DMSO-assisted iridium(III) complex (Ir1-DMSO), which can be applied as a "turn-on" photoluminescence (PL) probe for the selective detection and quantification of L-His/Ha. More importantly, Ir1-DMSO exhibited good sensitivity, high selectivity, and anti-interference capability for L-His/Ha/His-containing proteins, which is advantageous due to its simple fabrication and low technical demands. This was attributed to the reaction of Ir1-DMSO with imidazole and amino groups of L-His/Ha. Furthermore, we show the utility of Ir1-DMSO as a PL imaging agent in cultures of *E. coli* and *S. aureus*. Considering its diversity of composition and structural flexibility, it can be extended to other solvents and Ir-ligand complexes for various analyses based on specific molecular recognition sensing platforms.

Received 30th July 2024
Accepted 3rd September 2024

DOI: 10.1039/d4ay01431f

rsc.li/methods

Introduction

Amino acids serve as the essential building blocks of protein molecules and play a crucial role in various life activities and processes.[1] Histidine (His), a semi-essential amino acid, is characterized by its unique imidazole group. Additionally, His functions as a key neurotransmitter in numerous physiological processes.[2,3] A deficiency or excess of His in the human body can lead to a range of diseases. His-related metabolites include several biologically active substances, such as histamine (Ha), *N*-acetylhistamine (Ace), imidazole-4-acetate (ImA), and imidazole-propionic acid (ImP).[4] Abnormal levels of His and its metabolites can cause a variety of diseases.[5,6] For example, abnormal His levels are associated with chronic nephropathy, Friedreich ataxia, Parkinson's disease, inflammatory intoxication, asthma and advanced cirrhosis.[7,8] Excessive amounts of Ha can cause allergic reactions, such as mouth burning, flushing, nausea, headache, *etc.*[9] Consequently, monitoring His and its metabolites is closely linked to our physiological well-being. Developing straightforward and efficient methods for detecting His and its metabolites holds significant value for the early diagnosis of specific diseases.

In recent years, several methods such as colorimetry,[10–14] fluorimetry,[15–18] and electrochemical[19,20] methods have been explored for the detection of His or Ha. Optical sensors based on small molecule dyes, due to their sensitivity, simplicity and convenience, have been widely used in the determination of amino acids.[21,22] Recently, several iridium(III) complexes have been reported as luminescent probes for detecting chlorinated solvents,[23] bovine serum albumin (BSA),[24] picric acid,[25] hydrogen sulfide,[26] lipopolysaccharides,[27] and so on. In addition, several iridium(III) complexes have been reported for the detection of His. For example, Wang *et al.* introduced a His-specific $[Ir(ppy)_2(CH_3CN)_2]OTf$ complex (where ppy stands for 2-phenylpyridine and OTf denotes triflate) for cell imaging research.[28] Zhang *et al.* reported a tripyridyl cyclometallized iridium(III) complex containing benzoate as a two-photon fluorescent probe for imaging nuclear His.[29] Sarkar *et al.* developed a heterobimetallic complex containing Ir(III) and Pt(II) as a sensor for His and as a staining agent for His-rich proteins.[30] Sarkar *et al.* developed two complexes, IrL1 and IrL2, which were confirmed to function as switch-on fluorescent probes for detecting His or His-containing proteins.[31] However, because the chemical structures of His and its metabolites are very similar, the simple and efficient selective detection of these

[a]*School of Medical Engineering, Haojing College of Shaanxi University of Science & Technology, Xianyang 712046, Shaanxi, PR China*

[b]*Co-construction Collaborative Innovation Center for Chinese Medicine Resources Industrialization by Shaanxi & Education Ministry, Shaanxi University of Chinese Medicine, Xianyang, 712083, Shaanxi, PR China. E-mail: 1501034@sntcm.edu.cn*

† Electronic supplementary information (ESI) available. See DOI: https://doi.org/10.1039/d4ay01431f

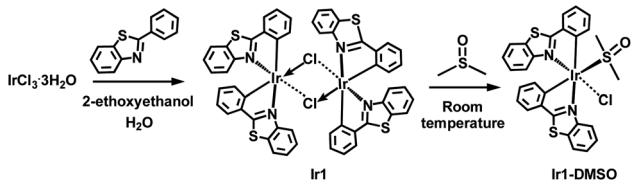

Fig. 1 Synthetic route of Ir1 and Ir1-DMSO.

compounds, especially in complex environments, remains a great challenge.

In this work, we anticipated that the complex would display weak or negligible emission. In living systems, it can covalently bond to endogenous L-His or His-rich proteins *via* a substitution reaction with the dimethyl sulfoxide (DMSO) ligand, resulting in enhanced luminescence. Iridium(III) complexes with outstanding PL activity were designed and synthesized, enabling their use as sensors.

Therefore, we designed a new DMSO-assisted iridium(III) complex, $Ir(bt)_2(DMSO)Cl$ (where bt = 2-phenylbenzothiazole, Ir1-DMSO, as illustrated in Fig. 1), and examined the coordination ability of Ir1-DMSO and L-His as well as Ha using photoluminescence (PL) techniques. The highly specific and selective reaction of Ir1-DMSO with L-His was further explored using L-His-related metabolites as interference objects. The analytical performance for detecting L-His further proved that the interaction between Ir1-DMSO and L-His can also be applied for detecting L-His-containing proteins.

Experimental

Chemicals and materials

$IrCl_3 \cdot 3H_2O$ and the bt compound were acquired from J&K Scientific Ltd. (China). L-His, Ha, Imp, Ace, Ima, and various other amino acids were obtained from Tokyo Chemical Industry Co., Ltd. (Japan). Four polypeptides were obtained from Apeptide Co., Ltd. (China). Phosphate-buffered saline (10 mM PBS, pH 7.4) was acquired from HyClone Company (USA). All chemicals were of analytical grade and did not require further purification, with Millipore Milli-Q water (18.2 MΩ cm) used for the experiments.

Synthesis of Ir1-DMSO

Firstly, Ir1 was synthesized according to reported procedures.[32] The major peak at $m/z = 613.0378$ in the mass spectra (Fig. S1†) should be ascribed to $[Ir(bt)_2]^+$ (calculated, 613.0384). We found that Ir1 can react with DMSO at room temperature to produce Ir1-DMSO. 5 mL of DMSO was added to 3.24 mg of Ir1 and the mixture was stirred continuously at room temperature until Ir1 was completely dissolved to obtain an orange red Ir1-DMSO (about 1 mM) solution. The characterization of Ir1-DMSO was carried out by electrospray ionization with high-resolution mass spectrometry. As shown in Fig. S2,† the characteristic peak centered at m/z 691.0515 was ascribed to Ir1-DMSO (calculated, 691.0523).

Fourier transform infrared spectroscopy (FTIR)

The samples were mixed with dry KBr powder and mechanically pressed to form a disc. Scans of the samples were recorded at a resolution of 1.5 cm^{-1} in the frequency range of 3400–400 cm^{-1}. The FTIR spectra of DMSO, Ir1, and Ir1-DMSO were recorded (Fig. S3†). Two new bands at 2914 cm^{-1} and 2998 cm^{-1} in Ir1-DMSO were assigned to the $-CH_3$ groups of the DMSO ligand. In addition, the FTIR spectra of Ir1-DMSO showed a band at 1044 cm^{-1}, which is related to the valence vibrations of the (S=O) bonds of the coordinated DMSO molecule.[33] The stretching vibrations bands of DMSO (C–S) = 710–570 cm^{-1} overlap with the bands of Ir1-DMSO.[34] Therefore, the structure of Ir1-DMSO is similar to that reported recently by Qian *et al.*, who confirmed through single-crystal X-ray crystallography that the structure of Ir-DMSO is orthogonal, with the Ir atom coordinated to the N atoms of the ligands, as well as to the S atom of DMSO and the Cl anion ligand.[35]

PL measurements

A volume of 0.005 mL of 1 mM Ir1-DMSO was mixed with 0.995 mL of 10 mM L-His or other samples at various concentrations and incubated at 37 °C for 30 min. PL spectra were obtained using a fluorescence spectrophotometer (Horiba JY, fluorolog-3, Japan) in the 480–700 nm range, with an excitation wavelength of λ_{ex} = 325 nm. PL quantum yields (Φ_{PL}) were measured on a Fluorolog-3 fluorescence spectrophotometer.

Bacterial imaging

The experimental procedures are outlined as follows: first, suitable amounts of *Escherichia coli* (*E. coli*) and *Staphylococcus aureus* (*S. aureus*) were collected using an inoculation loop and transferred to a shaking tube containing 2 mL of the Luria–Bertani (LB) liquid medium. The bacteria were incubated for 6 h in a thermostatic bacterial culture incubator to maintain them in the logarithmic growth phase. An appropriate volume of the bacterial suspension liquids was then centrifuged. The supernatants were discarded, and the bacteria were resuspended in an equal volume of PBS solution, repeating this process three times. Finally, the bacterial solutions were mixed thoroughly, and the OD600 absorbance was measured to be 0.5, corresponding to a bacterial concentration of approximately 1×10^8 CFU mL^{-1}. A volume of 0.1 mL of this bacterial suspension liquid was added to 0.9 mL of PBS solution, resulting in 1×10^7 CFU mL^{-1}. Subsequently, 5 μL of Ir1-DMSO were added to this suspension liquid for imaging *via* confocal laser scanning microscopy (CLSM, Olympus, Japan).

Results and discussion

The UV-vis absorption spectrum of Ir1-DMSO in DMSO/H_2O (1 : 99, v/v) shows intense ligand-centred absorption bands in the region of 200–350 nm (Fig. 2a), similar to that of a typical Ir(III) complex.[34,36] Ir1-DMSO exhibits weak PL emission at 575 nm under 325 nm excitation in DMSO/H_2O (5/95, v/v). To avoid the effect of DMSO on the luminescence performance of Ir1, we conducted a luminescence study on the chromogenic effect of

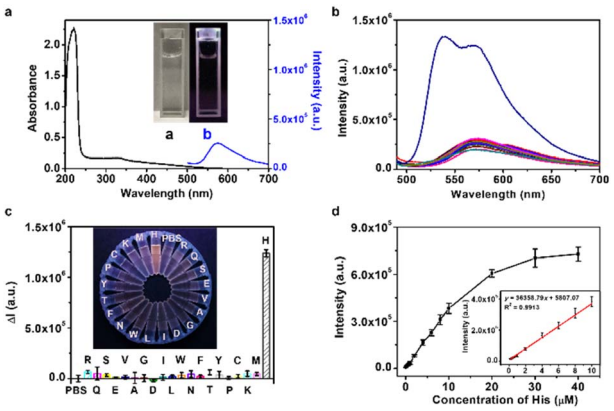

Fig. 2 (a) UV-vis absorption spectra of Ir1-DMSO in DMSO/PBS buffer solution (pH = 7.4, 5/95, v/v). (b) PL emission spectra and (c) relative emission intensity of Ir1-DMSO in the presence of 20 amino acids (50 μM). $\Delta I = I - I_0$, I and I_0 represents the PL intensity of Ir1-DMSO with or without various amino acids, λ_{ex} = 325 nm, λ_{em} = 538 nm. (d) The linearity between the PL intensity of Ir1-DMSO and the concentration of L-His (0.2–40 μM) at 540 nm.

the Ir1 solvent. The results showed that the volume of DMSO did not affect the luminescence performance of Ir1 (Fig. S4†).

Inspired by the specific luminescent properties of $[Ir(ppy)_2(solv)_2]^+$ (solv = H_2O or CH_3CN) for L-His/His-rich proteins,[37] here we investigated interactions between Ir1-DMSO and biomolecules including amino acids or proteins. The interactions of Ir1-DMSO with various amino acids were examined in the solution. As shown in Fig. 2b, in the presence of amino acids other than L-His, Ir1-DMSO exhibited a weak orange-red emission at a maximum wavelength of 575 nm. However, when L-His was present, the PL emission spectrum of Ir1-DMSO showed a shoulder peak, with a strong new peak appearing at 538 nm. A significant enhancement in the orange-red PL emission of L-His (about 14-fold) was observed, while the PL emission of Ir1-DMSO remained largely unchanged for the other 19 amino acids (Fig. 2c), including L-arginine, L-glutamine, L-serine, L-glutamic, L-valine, L-alanine, L-glycine, L-asparagine, L-isoleucine, L-leucine, L-tryptophan, L-aspartic, L-phenylalanine, L-threonine, L-tyrosine, L-proline, L-cysteine, L-lysine, and L-methionine. In order to explain the binding of L-His with the Ir1-DMSO in the presence of other interfering amino acids. As shown in Fig. S5,† the PL intensity of Ir1-DMSO in recognizing L-His was not affected by the presence of excess of other amino acids. These results demonstrated that Ir1-DMSO can be used for the highly selective detection of L-His without interference from other amino acids, making it a novel composite luminescent probe.

Kinetic experiments were optimized by detecting the PL emission intensity of Ir1-DMSO with L-His at different

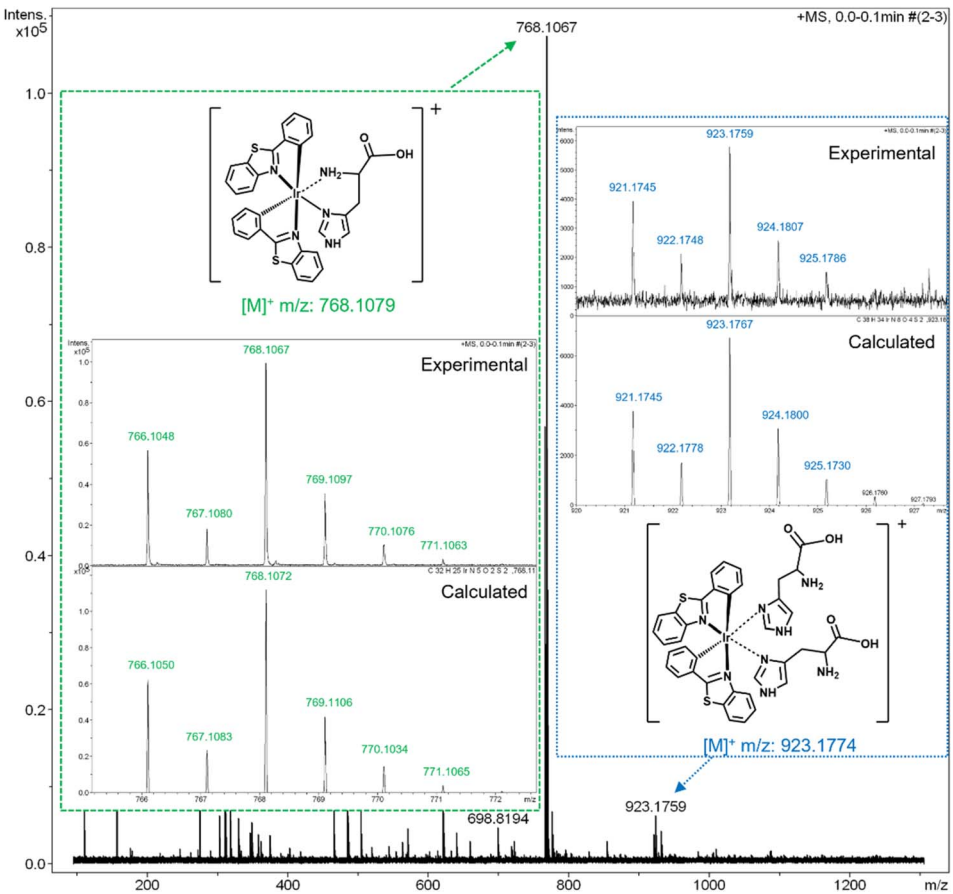

Fig. 3 Mass spectra of Ir1-DMSO experimental and calculated spectra of peak in the presence of 5 equivalents of L-His.

incubation times (Fig. S6†). Initially, before the addition of L-His (about 200 s), the PL intensity of Ir1-DMSO could be detected. After injecting 50 μM L-His, PL intensity (10 μM Ir1-DMSO) first increased during the first 20 min and then stabilized as the incubation time continued. The Φ_{PL} was measured to be 1.65% for Ir1-DMSO, and it significantly increased to 22.73% for Ir1-DMSO in the presence of L-His. The PL intensity based detection method for monitoring L-His variation was assessed based on changes in PL intensity. As the concentration of L-His increased from 0.2 to 40 μM, the PL intensity also rose accordingly (Fig. 2d). The L-His concentration (0.2 μM to 20 μM) exhibited a linear relationship with the PL intensity at 538 nm. The linear equation obtained was $y = 40\,165.86x + 4171.9055$ (mM, $R^2 = 0.9913$), with a detection limit of 0.08 μM. There may be a coordination reaction occurring between L-His and Ir1-DMSO, which is further supported by the mass spectra (MS) of Ir1-DMSO with and without L-His as a model. As illustrated in Fig. 3, after the addition of 5 equivalents of L-His, two characteristic peaks centred at m/z 768.1067 and 923.1759 were observed. These peaks correspond to Ir1-His (calculated, 768.1079) and Ir1-His2 (calculated, 923.1774), which were products resulting from the coordination reaction between $[Ir(bt)_2]$ and L-His. To further explore the binding mechanism of the proposed Ir1-His complexes, Ir1-DMSO, L-His, and Ir1-His were characterized by FTIR (Fig. S7†). The stretching vibrations observed at approximately 3037 cm^{-1} in the FTIR spectrum of L-His may be assigned to N–H symmetric stretches or the presence of protonated NH_2 groups.[38] L-His exhibited the characteristic bands of the imidazole ring at 1464 cm^{-1}.[39] The bands at 1639 cm^{-1} and 1508 cm^{-1} could be assigned to δ(NH) and ν(C=N) frequencies, respectively. The shape and position of the ν(C=N) bands indicate changes in the Ir1-His complex, suggesting the formation of Ir1–N=C.[40] Furthermore, the disappearance of the band at 1044 cm^{-1} in the Ir1-His complex may be due to the replacement of DMSO in Ir1-DMSO by L-His. The binding stoichiometry between Ir1-DMSO and L-His was determined using the Job plot experiment. Based on this continuous titration approach and PL measurements, the maximum mole fraction of Ir1-DMSO with L-His was 0.54 (Fig. S8†), indicating a 1.2 : 1 stoichiometric ratio.

To explore the practical applicability of Ir1-DMSO complexes for L-His detection under real conditions, we studied the effect of pH on the complexes in the absence or presence of L-His (Fig. S9†). The PL intensity of the complexes in the absence of L-His showed no significant change in a wide range of pH from 4.0 to 10.0, implying the good stability of Ir1-DMSO and its reliability for L-His detection. The PL intensity of Ir1-DMSO complexes was enhanced by the presence of L-His within the pH range of 4.0 to 10.0. We observed a slight increase in the PL intensity of Ir1-DMSO with increasing acid strength in the presence of L-His, which may be due to the protonation of the negatively charged carboxylic acid group present in L-His at acidic pH. Comparison of the analytical performance of Ir1-DMSO for the detection of L-His indicates good sensitivity and selectivity for the L-His assay, as illustrated in Table S1.† These results demonstrated that Ir1-DMSO can be successfully applied as a sensitive probe to accomplish the high selective PL based detection of L-His.

To further validate the selectivity of Ir1-DMSO for L-His, a metabolite with a similar structure to L-His was selected as a challenge, with its structure illustrated in Fig. 4a. The PL emission spectra are shown in Fig. 4b, where we can observe the effects of adding 50 μM of L-His and each of its four metabolites separately. The PL intensity significantly increased in the presence of L-His and Ha, while ImA, ImP, and Ace showed barely any change. When Ha was added to the Ir1-DMSO solution, the PL spectrum was notably enhanced, resulting in a broad peak with a main peak at 550 nm. By comparing the structure of L-His with that of the metabolite, we found that the PL spectrum of Ir1-DMSO displayed a double shoulder with a main peak at 538 nm when both amino and carboxyl groups were present. In contrast, when only the amino group was present, the PL spectrum of Ir1-DMSO exhibited a double broad peak with a main peak at 550 nm. However, the PL spectra of Ir1-DMSO did not change significantly when only carboxyl groups or amides were present. This was attributed to the reaction of Ir1-DMSO with the imidazole and amino groups of L-His/Ha.

To further demonstrate the role of the carboxyl group in the reaction between Ir1-DMSO and L-His, four His-free polypeptide chains (P1: DPKKRKV, P2: DVQRKRLMP, P3: KVQRKRQKLMP, and P4: KLTRAQRARKNRT), as well as BSA (607 AA, with 17 His

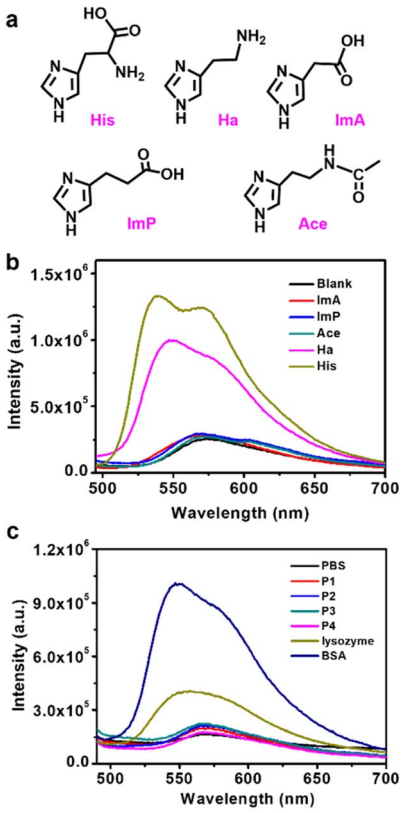

Fig. 4 (a) Structures of L-His, Ha, ImA, ImP, and Ace. (b) PL emission spectra of Ir1-DMSO toward L-His, Ha, ImA, ImP, and Ace. (c) PL emission spectra of Ir1-DMSO toward 10 μM P1–P4, BSA, and HSA.

residues) and lysozyme (147 AA, with one His residue) were selected. The PL emission spectra of Ir1-DMSO in relation to P1–P4, BSA, and lysozyme are shown in Fig. 4c. The spectral intensity of Ir1-DMSO was significantly enhanced when mixed with BSA and slightly enhanced when mixed with lysozyme, with the main peak at 550 nm. This enhancement may be attributed to the lack of free carboxyl groups in the His residues of the proteins. In contrast, no change in PL intensity was observed when Ir1-DMSO was mixed with any of the four peptides without L-His, further demonstrating the highly specific selective reaction of Ir1-DMSO with L-His.

Considering the use of Ir1-DMSO for detecting L-His and Ha/His-proteins through PL emission, optical microscopy further verified the presence of bacteria containing His-proteins. *E. coli* is a typical Gram-negative bacterium and is the most important and abundant bacterium found in the intestines of humans and many animals. Importantly, *E. coli* contains various proteases with L-His residues.[40–45] Furthermore, *S. aureus*, another typical Gram-negative bacterium, also contains various proteases with L-His residues.[46,47] Therefore, we chose these two bacteria as targets for imaging to demonstrate the selectivity of Ir1-DMSO towards L-His. As shown in Fig. 5, after 30 min of incubation with Ir1-DMSO, a strong emission was distinctly observed under a CLSM, whereas the bacteria lacking Ir1-DMSO appeared blank. The bright- and dark-field CLSM imaging of the bacteria using Ir1-DMSO probes exhibited no background noise. This approach allowed for clear visibility of the bacteria without the need for any washing steps, minimizing bacterial loss during the washing process and streamlining the imaging procedure. Consequently, the characteristics of Ir1-DMSO render it more suitable and advantageous than conventional fluorescence dyes for bacterial imaging.

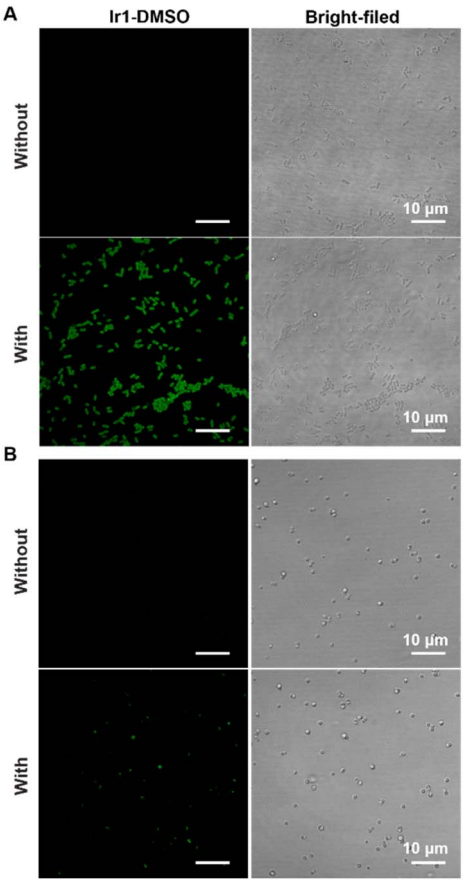

Fig. 5 CLSM images of (A) *E. coli* and (B) *S. aureus* treated with or without Ir1-DMSO (30 min), respectively.

Conclusions

In conclusion, we successfully designed and synthesized a DMSO-assisted iridium(III) complex (Ir1-DMSO), which serves as a "turn on" PL probe for the selective detection of L-His/Ha. When L-His was present, the PL emission spectrum of Ir1-DMSO showed a shoulder peak, accompanied by a strong new peak at 538 nm. A linear correlation ($R^2 = 0.9913$) was established between the concentration of Ir1-DMSO and L-His in the range of 0.2–20 μM, with a detection limit of 0.08 μM. Notably, Ir1-DMSO demonstrated excellent sensitivity, high selectivity, and strong anti-interference capabilities for L-His/Ha and L-His-containing proteins, making it advantageous due to its simple fabrication and low technical requirements. This performance is attributed to the interaction of Ir1-DMSO with the imidazole and amino groups of L-His/Ha. Additionally, we demonstrated the effectiveness of Ir1-DMSO as a PL imaging agent in cultures of *E. coli* and *S. aureus*. This study highlights Ir1-DMSO as a promising alternative "turn on" PL probe for detecting L-His. Given its compositional diversity and structural flexibility, it can be adapted for use with other solvents and Ir-ligand complexes for various analyses based on specific molecular recognition sensing platforms.

Data availability

The authors confirm that the data supporting the findings of this study are available within the article and its ESI.†

Conflicts of interest

There are no conflicts to declare.

Acknowledgements

This work was financially supported by the General Science Foundation of Education Department of Shaanxi Provincial Government (23JK0404) and the Doctoral Science Foundation of Shaanxi University of Chinese Medicine (306-171020323004).

Notes and references

1 N. P. Rao, C. M. Vaishnavi, M. S. Kumar, S. Vishnu, B. Mukherjee, N. Karthik, G. Dutta and A. K. Das, *Anal. Methods*, 2023, **15**, 2546.
2 T. Chen, L. Yin, C. Huang, Y. Qin, W. Zhu, Y. Xu and X. Qian, *Biosens. Bioelectron.*, 2015, **66**, 259–265.

3 Y. Cai, J. Wang, C. Liu, S. Yang, Y. Zhang and A. Liu, *Chem. Commun.*, 2020, **56**, 11637.
4 M. Qian, Y. Liu, H. Huo, M. Li, C. Zhang and H. Qi, *Anal. Chem.*, 2024, **96**, 446–454.
5 Z. Zhang, L. Wang, G. Li and B. Ye, *Analyst*, 2017, **142**, 1821.
6 H. S. Al-mashriqi, M. Cai, S. Qi and H. Zhai, *J. Fluoresc.*, 2023, **33**, 697–706.
7 X. Lin, Z. Hao, H. Wu, M. Zhao, X. Gao, S. Wang and Y. Liu, *Microchim. Acta*, 2019, **186**, 648.
8 K. Liu, G. Du, L. Ye and L. Jiang, *Sens. Actuators, B*, 2019, **284**, 55–62.
9 S. Xu, F. Wu, F. Mu and B. Dai, *J. Electroanal. Chem.*, 2022, **908**, 116088.
10 R. B. Unabia, R. L. D. Reazo, R. B. P. Rivera, M. A. Lapening, J. L. Omping, R. M. Lumod, A. G. Ruda, N. L. B. Sayson, G. Dumancas, R. M. Malaluan, A. A. Lubguban, G. C. Petalcorin, R. Y. Capangpangan, F. S. Latayada and A. C. Alguno, *ACS Omega*, 2024, **9**, 17238–17246.
11 L. Zhu, J. Zhang, H. Zhang, M. Zhang and J. Wang, *Sens. Actuators, B*, 2024, **412**, 135819.
12 Y. Uppa, S. Srijaranai and S. Chanthai, *Anal. Sci.*, 2021, **37**, 1741–1748.
13 H. Tavallali, O. Espergham, G. Deilamy-Rad, M. A. Karimi, S. Rostami and A.-R. Rouhani-Savestani, *Anal. Biochem.*, 2020, **604**, 113811.
14 Y. S. Kim, G. J. Park, S. A. Lee and C. Kim, *RSC Adv.*, 2015, **5**, 31179.
15 R. Zhao, X. Chai, C. Dong, S. Shuang and Y. Guo, *Microchem. J.*, 2024, **199**, 109960.
16 Y. Fu, H. Yang, L. Dong, F. Wang, X. Chen and J. Wang, *Spectrochim. Acta A.*, 2024, **307**, 123619.
17 G. Wu, Z. Ding, X. Dou, Z. Chen and J. Xie, *Spectrochim. Acta A.*, 2024, **317**, 124452.
18 J. Xiao, L. Song, M. Liu, X. Wang and Z. Liu, *Inorg. Chem.*, 2020, **59**, 6390–6397.
19 M. Zhang, M. Qian, H. Huang, Q. Gao, C. Zhang and H. Qi, *J. Electroanal. Chem.*, 2022, **920**, 116578.
20 Y. Zhou, K. Xie, L. Kong, F. Chen and D. Sun, *J. Electroanal. Chem.*, 2017, **799**, 122–125.
21 B. Das and P. Gupta, *Coordin. Chem. Rev.*, 2024, **504**, 215656.
22 L. C.-C. Lee and K. K.-W. Lo, *Chem. Rev.*, 2024, **124**, 8825–9014.
23 N. Kashyap, M. Rabha, S. K. Patra, B. Sen, S. K. Sheet, K. Baruah and S. Khatua, *Cryst. Growth Des.*, 2024, **24**, 3615–3631.
24 Q. Chen, S. Sheth, Y. Zhao and Q. Song, *Anal. Methods*, 2019, **11**, 3033–3040.
25 M. Rabha, D. L. Lyngkhoi, S. K. Patra and S. Khatua, *Inorg. Chem. Front.*, 2024, **11**, 1434–1449.
26 X. Mu, W. Zhang, M. Li and F. Fu, *Sens. Actuators, B*, 2024, **401**, 134972.
27 A. Gautam, A. Gupta, P. Prasad and P. K. Sasmal, *Dalton Trans.*, 2023, **52**, 7843–7853.
28 X. Wang, J. Jia, Z. Huang, M. Zhou and H. Fei, *Chem.–Eur. J.*, 2011, **17**, 8028–8032.
29 Q. Zhang, X. Lu, H. Wang, X. Tian, A. Wang, Ho. Zhou, J. Wu and Y. Tian, *Chem. Commun.*, 2018, **54**, 3771–3774.
30 A. Sarkar, R. Kumar, B. Das, P. S. Ray and P. Gupta, *Dalton Trans.*, 2020, **49**, 1864–1872.
31 L. Hu, X. Chen, K. Yu, N. Huang, H. Du, Y. Wei, Y. Wu and H. Wang, *Spectrochim. Acta A.*, 2021, **262**, 120095.
32 H. Huang, S. Banerjee, K. Qiu, P. Zhang, O. Blacque, T. Malcomson, M. J. Paterson, G. J. Clarkson, M. Staniforth, V. G. Stavros, G. Gasser, H. Chao and P. J. Sadler, *Nat. Chem.*, 2019, **11**, 1041–1048.
33 A. I. Karelin, R. R. Kayumov and Y. A. Dobrovolsky, *Spectrochim. Acta A.*, 2019, **215**, 381–388.
34 A. A. Ksenofontov, G. B. Guseva, E. V. Antina, I. A. Khodov and A. I. Vyugin, *Sens. Actuators, B*, 2017, **251**, 858–868.
35 M. Qian, K. Wang, P. Yang, Y. Liu, M. Li, C. Zhang and H. Qi, *Chem. Biomed. Imaging*, 2024, DOI: **10.1021/cbmi.4c00042**.
36 R. Bevernaegie, S. A. M. Wehlin, E. J. Piechota, M. Abraham, C. Philouze, G. J. Meyer, B. Elias and L. Troian-Gautier, *J. Am. Chem. Soc.*, 2020, **142**, 2732–2737.
37 D. L. Ma, W. Wong, W. Chung, F. Chan, P. So, T. Lai, Z. Zhou, Y. Leung and K. Wong, *Angew. Chem., Int. Ed.*, 2008, **47**, 3735–3739.
38 X. Guo, R. Wang, B. Han, W. Shao, L. Chen and X. Feng, *Food Chem.*, 2024, **448**, 139070.
39 K. Shrivas, W. Naik, D. Kumar, D. Singh, K. Dewangan, T. Kant, S. Yadav, Tikeshwari and N. Jaiswal, *Microchem. J.*, 2021, **160**, 105597.
40 K. M. A. El-Nour, E. T. A. Salam, H. M. Soliman and A. S. Orabi, *Nanoscale Res. Lett.*, 2017, **12**, 231.
41 C. Li, M. Yu, Y. Sun, Y. Wu, C. Huang and F. Li, *J. Am. Chem. Soc.*, 2011, **133**, 11231–11239.
42 P. P. D. Nocera, F. Blasi, R. D. Lauro, R. Frunzio and C. B. Bruni, *Proc. Nati. Acad. Sci. USA*, 1978, **75**, 4276–4280.
43 T. Pourcher, H. K. Sarkar, M. Bassilana, H. R. Kaback and G. Leblanc, *Proc. Natl. Acad. Sci. U.S.A.*, 1990, **87**, 468–472.
44 C. A. Batt, A. C. Jamieson and M. A. Vandeyar, *Proc. Natl. Acad. Sci. U.S.A.*, 1990, **87**, 618–622.
45 G. Compain, C. Monsarrat, J. Blagojevic, K. Brillet, P. Dumas, P. Hammann, L. Kuhn, I. Martiel, S. Engilberge, V. Oliéric, P. Wolff, D. Y. Burnouf, J. Wagner and G. Guichard, *JACS Au*, 2024, **4**, 432–440.
46 B. E. Menzies and D. S. Kernodle, *Infect. Immun.*, 1994, **62**, 1843–1847.
47 C. M. Beetham, C. F. Schuster, M. Santiago, S. Walker and A. Gründling, *bioRxiv*, 2023, DOI: **10.1101/2023.07.25.550546**.

